Aaij, R. et al. (2012) First observation of the decay B0s→K∗0K∗0. Physics Letters B, 709 (1-2). pp. 50-58. ISSN 0370-2693

Physics Letters B 709 (2012) 50–58

Contents lists available at SciVerse ScienceDirect

Physics Letters B

www.elsevier.com/locate/physletb

First observation of the decay $B_s^0 \to K^{*0}\overline{K}^{*0}$ ☆

LHCb Collaboration

ARTICLE INFO

Article history:
Received 18 November 2011
Received in revised form 9 January 2012
Accepted 1 February 2012
Available online 4 February 2012
Editor: W.-D. Schlatter

ABSTRACT

The first observation of the decay $B_s^0 \to K^{*0}\overline{K}^{*0}$ is reported using 35 pb^{-1} of data collected by LHCb in proton–proton collisions at a centre-of-mass energy of 7 TeV. A total of 49.8 ± 7.5 $B_s^0 \to (K^+\pi^-)(K^-\pi^+)$ events are observed within ± 50 MeV/c^2 of the B_s^0 mass and 746 MeV/$c^2 < m_{K\pi} <$ 1046 MeV/c^2, mostly coming from a resonant $B_s^0 \to K^{*0}\overline{K}^{*0}$ signal. The branching fraction and the *CP*-averaged K^{*0} longitudinal polarization fraction are measured to be $\mathcal{B}(B_s^0 \to K^{*0}\overline{K}^{*0}) = (2.81 \pm 0.46(\text{stat.}) \pm 0.45(\text{syst.}) \pm 0.34(f_s/f_d)) \times 10^{-5}$ and $f_L = 0.31 \pm 0.12(\text{stat.}) \pm 0.04(\text{syst.})$.

1. Introduction

The decay $B_s^0 \to K^{*0}\overline{K}^{*0}$ is described in the Standard Model by loop (penguin) diagrams that contain a $b \to s$ transition. The partial width of the decay arises from three helicity amplitudes that, assuming no additional contributions from physics beyond the Standard Model, are determined by the chiral structure of the quark operators. Predictions obtained within the framework of QCD factorization [1] are $\mathcal{B}(B_s^0 \to K^{*0}\overline{K}^{*0}) = (9.1^{+11.3}_{-6.8}) \times 10^{-6}$ for the branching fraction and $0.63^{+0.42}_{-0.29}$ for the K^{*0} longitudinal polarization fraction. Predictions improve to $(7.9^{+4.3}_{-3.9}) \times 10^{-6}$ and $0.72^{+0.16}_{-0.21}$, respectively, when experimental input is used from $B \to K^*\phi$ [2,3]. The possibility to use $B_s^0 \to K^{*0}\overline{K}^{*0}$ for precision *CP*-violation studies to determine the phases β_s and γ of the CKM matrix [4] has been emphasized by several authors [5–8]. The U-spin related channel, $B^0 \to K^{*0}\overline{K}^{*0}$, a $b \to d$ transition, has been observed by BaBar [9], reporting a branching fraction of $(1.28^{+0.35}_{-0.30} \pm 0.11) \times 10^{-6}$ and $f_L = 0.80^{+0.10}_{-0.12} \pm 0.06$ with a signal yield of $33.5^{+9.1}_{-8.1}$ events. An upper limit for the $B_s^0 \to K^{*0}\overline{K}^{*0}$ branching fraction of 1.68×10^{-3} with 90% confidence level was reported by the SLD experiment [10].

We present in this Letter the first observation of the $B_s^0 \to K^{*0}\overline{K}^{*0}$ decay using pp collisions at $\sqrt{s} = 7$ TeV at the LHC. The data were collected during 2010 and corresponds to 35 pb^{-1} of integrated luminosity. LHCb has excellent capabilities to trigger and reconstruct beauty and charm hadrons, and covers the pseudorapidity region $2 < \eta < 5$. The tracking system consists of a 21 station, 1-metre long array of silicon strip detectors placed within 8 mm of the LHC beams. This is followed by a four layer silicon strip detector upstream of a 4 Tm dipole magnet. Downstream of the magnet are three tracking stations, each composed of a four-layer silicon strip detector in the high occupancy region near the beam pipe, and an eight layer straw tube drift chamber composed of 5 mm diameter straws outside this high occupancy region. Overall, the tracking system provides an impact parameter (IP)[1] resolution of 16 μm + 30 μm/p_{T} (GeV/c), and a momentum resolution σ_p/p below 8 per mille up to $100/mboxGeV/c$. Two ring imaging Cherenkov detectors, one upstream of the magnet, and a second just downstream of the tracking stations, together provide a typical kaon identification efficiency of 90%. The pion fake rate, over the momentum range from 3–100 GeV/c, is between 5 and 10 percent. Further downstream is a Preshower/Scintillating Pad Detector, an electromagnetic calorimeter, and a hadronic calorimeter. The LHCb spectrometer also features a large, five station muon system used for triggering on and identifying muons. A more detailed description of the LHCb detector can be found in [11].

To reduce the data rate from the LHC crossing rate to about 2 kHz for permanent storage, LHCb uses a two-level trigger system. The first level of the trigger, implemented in hardware, searches for either a large transverse energy (E_{T}) cluster in the calorimeters ($E_{\mathrm{T}} > 3.6$ GeV is a representative value during the 2010 run), or a single high transverse momentum (p_{T}) muon or di-muon pair in the muon stations.

Events passing the hardware trigger are read out and sent to a large computing farm, where they are analyzed using a software-based trigger [12]. The first stage of the software trigger relies on the selection of a single track with IP larger than 125 μm, $p_{\mathrm{T}} > 1.8$ GeV/c, $p > 12.5$ GeV/c, along with other track quality requirements. Events are subsequently analyzed by a second software stage, where the event is searched for 2, 3, or 4-particle vertices that are consistent with originating from b-hadron decays. The impact parameter χ^2 of the selected tracks (IPχ^2), defined

☆ © CERN for the benefit of the LHCb Collaboration.

[1] The impact parameter is the distance of closest approach between a particle's trajectory and its assumed production point.

0370-2693/ © 2012 CERN. Published by Elsevier B.V. All rights reserved.
doi:10.1016/j.physletb.2012.02.001

as the difference between the χ^2 of the primary vertex (PV) built with and without the considered track, is required to be greater than 16 with respect to any PV. The tracks are also required to have $p > 5$ GeV/c and $p_T > 0.5$ GeV/c. The B_s^0 decay vertex must have at least one track with $p_T > 1.5$ GeV/c, a scalar p_T sum of at least 4 GeV/c, and a corrected mass[2] between 4 and 7 GeV/c^2. Additional track and vertex quality cuts are also applied.

Events with large occupancy are slow to reconstruct and were suppressed by applying global event cuts to hadronically triggered decays. These included limits on the number of hits in the tracking detectors and scintillating pad detector.

2. Selection procedure and signal yield

To search for the decay process $B_s^0 \to K^{*0}(K^+\pi^-)\overline{K}^{*0}(K^-\pi^+)$ we applied a number of offline selection criteria. When a four-track secondary vertex is found, the reconstructed momentum of the B_s^0 candidate is used to calculate the smallest impact parameter with respect to all primary vertices in the event. Tracks are required to have $p_T > 500$ MeV/c, and a large impact parameter (IP$\chi^2 > 9$) with respect to the PV. The difference in the natural logarithm of the likelihoods of the kaon and pion hypotheses must be greater than 2 for K^+ and K^- candidates, and less than 0 for π^+ and π^- candidates. In addition, the $K^+\pi^-$ combinations[3] must form an acceptable quality common vertex (χ^2/ndf < 9), where ndf is the number of degrees of freedom in the vertex fit) and must have an invariant mass within ± 150 MeV/c^2 of the nominal K^{*0} mass (this is around ± 3 times its physical width [4]). The K^{*0} and $\overline{K}^{*0}$ candidates must have $p_T > 900$ MeV/c and the distance of closest approach between their trajectories must be less than 0.3 mm. The secondary vertex must be well fitted (χ^2/ndf < 5). Finally, the B_s^0 candidate momentum is required to point to the PV.

To improve the signal significance, a multivariate analysis is used that takes into account the properties of the $B_s^0 \to K^{*0}(K^+\pi^-)\overline{K}^{*0}(K^-\pi^+)$ signal, as well as those of the background. It is based on a geometrical likelihood (GL) [13,14] that uses the following set of variables as input:

- B_s^0 candidate impact parameter with respect to the closest primary vertex.
- Decay time of the B_s^0 candidate.
- Minimum impact parameter χ^2 of the four tracks with respect to all primary vertices in the event.
- Distance of closest approach between the two K^{*0} trajectories reconstructed from the pion and kaon tracks.
- p_T of the B_s^0 candidate.

For a given input sample, the above distributions are converted into a set of uncorrelated, Gaussian-distributed variables. Two vectors are defined for each event indicating its distance to the signal $\{S_i\}$ and to the background $\{B_i\}$ hypotheses by means of $\chi_S^2 = \sum S_i^2$ and $\chi_B^2 = \sum B_i^2$, where the index i runs over the five discriminating variables indicated above. The quantity $\Delta\chi^2 = \chi_S^2 - \chi_B^2$ is found to be a good discriminant between the two hypotheses and is used to construct the GL function in such a way that it is uniformly distributed in the range [0, 1] for signal events and tends to have low values for the background. The signal input is generated by EvtGen [15] and Pythia 6.4 [16] for the kinematic spectra, and the full detector simulation is based on GEANT4 [17].

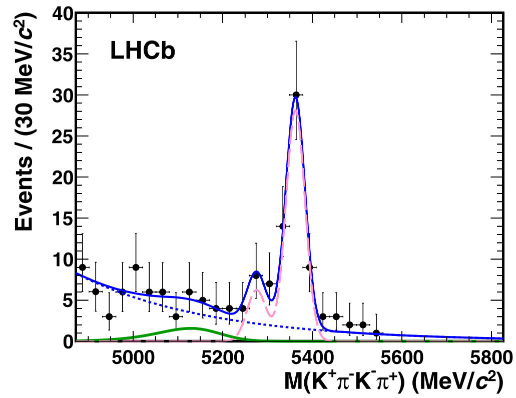

Fig. 1. Fit to the $K^+\pi^-K^-\pi^+$ mass distribution of selected candidates. The fit model (dashed pink curve) includes a signal component that has two Gaussian components corresponding to the B_s^0 and B^0 decays. The background is described as an exponential component (dotted blue) plus the parametrization indicated in the text (dash-dotted green). (For interpretation of the references to color in this figure legend, the reader is referred to the web version of this Letter.)

The GL selection requirement was determined by maximizing the signal significance. The GL was trained using a fully reconstructed $B_s^0 \to K^{*0}\overline{K}^{*0}$ simulation sample for the signal, and a selected background sample from the first 2 pb^{-1} of data, which is not used in the analysis. The requirement GL > 0.24, together with the above selection criteria, resulted in the mass spectrum in Fig. 1 for the selected $K^+\pi^-K^-\pi^+$ candidates. It is observed that the events with masses below the signal region have on average slightly higher GL values than those with masses above. This indicates the presence of a background from partially reconstructed B decays.

To describe the data, we have used a fit including two Gaussian probability density functions (PDFs) centered at the B^0 and B_s^0 masses respectively, a decreasing exponential and the following parametrization for partially reconstructed B-decays

$$AM'\left(1 - \frac{M'^2}{M_p^2}\right)\Theta\left(M_p - M'\right)e^{-k_p \cdot M'} \otimes G\left(M - M'; \sigma_p\right), \tag{1}$$

where Θ is the Heaviside-step function, $\otimes$ represents the convolution, M' is the variable over which the convolution integral is calculated, $G(M - M'; \sigma_p)$ is a Gaussian PDF with standard deviation σ_p and M_p and k_p are free parameters. The fit results are given in Table 1.

The measured signal yield in a window of ± 50 MeV/c^2 around the B_s^0 mass is $N_{K^+\pi^-K^-\pi^+} = 49.8 \pm 7.5$(stat.). The width of the B_s^0 peak is in good agreement with the LHCb resolution measured in decays with similar kinematics such as $B_s^0 \to J/\psi\phi$. The significance of the B_s^0 signal was determined to be 10.9σ by comparing the log of the likelihood between the models with and without signal. When doing this test, the mass and width of the B_s^0 and B^0 mesons were fixed to those obtained from independent LHCb measurements of $B_s^0 \to J/\psi\phi$ and $B^0 \to J/\psi K^{*0}$, respectively. The peak at the B^0 mass, though not significant, is compatible with the $B^0 \to K^{*0}\overline{K}^{*0}$ branching fraction measured by BaBar [9].

As the K^{*0} meson is light compared to the B_s^0 meson, the invariant masses of the three-body systems $K^+K^-\pi^\pm$ and $K^+\pi^-\pi^\pm$ are rather high, above those of the charmed hadrons. This kinematically excludes the possibility of contamination from $b \to c$ decays with very short charm flight distance, in particular $B_s^0 \to D_s^-\pi^+$.

After subtraction of the non-B_s^0 component, the $K^+\pi^-$ mass combinations were studied, within a ± 50 MeV/c^2 window of

[2] The corrected mass is related to the invariant mass m, as $m_{corr} = \sqrt{m^2 + |p_{T\,miss}|^2} + |p_{T\,miss}|$, where $p_{T\,miss}$ is the missing momentum transverse to the B_s^0 direction.

[3] This expression refers hereafter to both charge combinations: $K^+\pi^-$ and $K^-\pi^+$.

Table 1
Fitted values of the model parameters for the mass spectrum, as described in the text. N_s and N_d are the number of events for the B_s^0 and B^0 signals, μ_s is the fitted mass value for the B_s^0 signal and σ is the Gaussian width. The mass difference between B_s^0 and B^0 was fixed to its nominal value [4]. N_b is the number of background events in the full mass range (4900–5800 MeV/c^2), and c_b is the exponential parameter in the fit. M_p, σ_p and k_p are the parameters of Eq. (1). Finally, f_p is the fraction of the background associated with Eq. (1).

Parameter	Value
N_s	50.1 ± 7.5
N_d	11.2 ± 4.3
μ_s (MeV/c^2)	5362.5 ± 4.8
σ (MeV/c^2)	21.2 ± 3.3
N_b	90 ± 10
c_b (10^{-3} (MeV/c^2)$^{-1}$)	−3.37 ± 0.55
k_p (10^{-2} (MeV/c^2)$^{-1}$)	5.5 ± 5.3
f_p	$0.06^{+0.24}_{-0.05}$
M_p (MeV/c^2)	5170 ± 170
σ_p (MeV/c^2)	37 ± 23

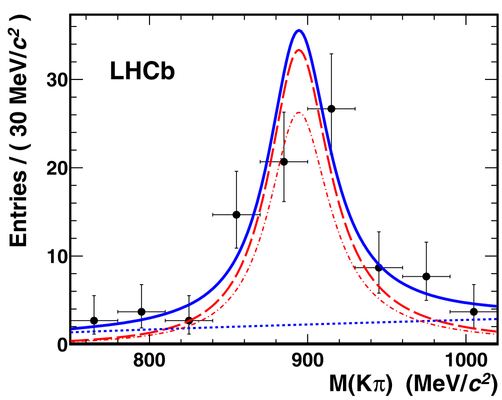

Fig. 2. Background subtracted $K^+\pi^-$ and $K^-\pi^+$ combinations for selected candidates within a ±50 MeV/c^2 window of the B_s^0 mass. The solid blue line shows the projection of the 2D fit model described in the text, indicating the $K^{*0}\overline{K}^{*0}$ yield (dashed–dotted red line) and a nonresonant component (blue dotted line), assumed to be a linear function times the two-body phase space. The dashed red line indicates the overall $B_s^0 \to K^{*0}X$ contribution. (For interpretation of the references to color in this figure legend, the reader is referred to the web version of this Letter.)

the B_s^0 signal, by means of a maximum likelihood fit in the $(m_{K^+\pi^-}, m_{K^-\pi^+})$ plane. Three components are included in the fit, namely a double Breit–Wigner distribution describing $B_s^0 \to K^{*0}\overline{K}^{*0}$ production, a symmetrized product of a Breit–Wigner and a nonresonant linear model adjusted for phase space in the $K^+\pi^-$ mass, and a double nonresonant component. The fit result, as shown in Fig. 2, gives $(62 \pm 18)\%$ $K^{*0}\overline{K}^{*0}$ production. The remainder is the symmetrized Breit–Wigner/nonresonant model.

The shape of the background mass distribution was extracted from a fit to the $K^+\pi^-$ mass spectrum observed in two 400 MeV/c^2 wide sidebands below and above the B_s^0 mass. The number of background events to be subtracted was determined from the results in Table 1. The sizable K^{*0} contribution present in this background was taken into account.

A model for $B_s^0 \to K^{*0}\overline{K}^{*0}(1430)$, representing a broad scalar state interfering with $B_s^0 \to K^{*0}\overline{K}^{*0}$ was also studied in the available $K^+\pi^-$ mass range of ±150 MeV/c^2 around the K^{*0} mass. The small number of events made it impossible to measure precisely the size of such a contribution for all values of the interfering phase. However, for values of the phase away from $\pi/2$ and $3\pi/2$ it was determined to be below 12%. Further study of this issue requires a larger data sample.

Table 2
Selection and trigger efficiencies obtained from simulation. The observed yield found for the signal and control channels in the full mass range are also indicated. The efficiency errors are statistical, derived from the size of the simulated samples.

	ϵ^{sel} (%)	ϵ^{trig} (%)	Yield
$B_s^0 \to K^{*0}\overline{K}^{*0}$	0.370 ± 0.005	37.12 ± 0.39	42.5 ± 6.7
$B^0 \to J/\psi K^{*0}$	0.547 ± 0.007	31.16 ± 0.63	657 ± 27
Ratio	0.678 ± 0.013	1.191 ± 0.027	0.065 ± 0.011

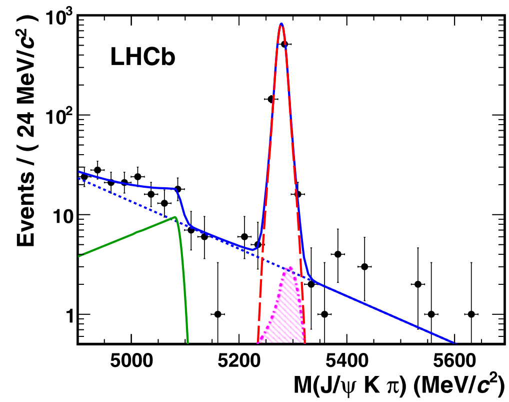

Fig. 3. Fit to the mass distribution of selected $B^0 \to J/\psi K^{*0}$ events. The dashed red curve is the Gaussian component for the B signal. The green dashed–dotted line accounts for partially reconstructed $B \to J/\psi X$ (see Eq. (2)). The pink hatched region accounts for a possible $B_s^0 \to J/\psi\phi$ contamination, parametrized as a sum of two Crystal–Ball functions [20]. The combinatorial background is parametrized as an exponential and indicated as a blue dotted line. (For interpretation of the references to color in this figure legend, the reader is referred to the web version of this Letter.)

3. Selection of the control channel

The branching fraction measurement of $B_s^0 \to K^{*0}\overline{K}^{*0}$ is based upon the use of a normalization channel with a well measured branching fraction, and knowledge of the selection and trigger efficiencies for both the signal and normalization channels. We chose $B^0 \to J/\psi K^{*0}$, with $J/\psi \to \mu^+\mu^-$, for this purpose. This decay has a similar topology to the signal, allowing the selection cuts to be harmonized, and it is copiously produced in the LHCb acceptance. The presence of two muons in the final state means that $B^0 \to J/\psi K^{*0}$ tends to be triggered by a muon rather than a hadron, leading to a higher efficiency than for $B_s^0 \to K^{*0}\overline{K}^{*0}$. The differences in the trigger can be mitigated by only considering $B^0 \to J/\psi K^{*0}$ candidates where the trigger decision was not allowed to be based on muon triggers that use tracks from the decay itself.

The offline selection criteria for $B^0 \to J/\psi K^{*0}$ were designed to mimic those of $B_s^0 \to K^{*0}\overline{K}^{*0}$. In particular, all cuts related to the B_s^0 vertex definition were kept the same. We also used the same GL as for the signal.

The overall detection efficiency was factorized as $\epsilon^{sel}\epsilon^{trig}$. The first factor ϵ^{sel} is the probability of the generated tracks being accepted in the LHCb angular coverage, reconstructed, and selected. The second factor ϵ^{trig} defines the efficiency of the trigger on the selected events. Both are indicated in Table 2, as calculated from Monte Carlo simulation, along with the number of selected events. Note that our measurement depends only on the ratios of efficiencies between signal and control channels.

The event yield for the selected data was determined from a fit to the $J/\psi K^+\pi^-$ invariant mass spectrum as shown in Fig. 3. In this fit, a constrained J/ψ mass was used in order to improve the B^0 mass resolution and therefore background rejection.

A component for the particular background source $B_s^0 \to J/\psi\phi$, with $\phi \to K^+K^-$, was included in the fit, with a parametrization defined from simulation, yielding the result 8 ± 8 events. The complete suppression of this background was subsequently confirmed using the Armenteros–Podolanski [18] plot for the K^{*0} kinematics. The fit model also includes a Gaussian signal for the B^0 meson, and a combinatorial background component parameterized with an exponential function and an additional component to account for partially reconstructed $B \to J/\psi X$ [19]. This partially reconstructed component can be described as

$$\rho(M, \overline{M}, \mu, \kappa) \propto \begin{cases} e^{-\frac{1}{2}(\frac{M-\overline{M}}{\kappa})^2} & \text{if } M > \mu, \\ e^{-\frac{1}{2}(\frac{\mu-\overline{M}}{\kappa})^2 + \frac{(\overline{M}-\mu)(M-\mu)}{\kappa^2}} & \text{if } M \leqslant \mu, \end{cases} \tag{2}$$

where the parameters μ, κ and $\overline{M}$ are allowed to float. The fitted signal according to this model is indicated in the third column of Table 2.

A small fraction of the selected sample contains two alternative candidates for the reconstructed event, which share three of the particles but differ in the fourth one. Those events, which amount to 3.8% (3.7%) in the signal (control) channels, were retained for the determination of the branching fraction.

4. Analysis of K^{*0} polarization

The four-particle $K^+\pi^-K^-\pi^+$ angular distribution describing the decay of B_s^0 into two vector mesons ($K^{*0} \to K^+\pi^-$ and $\overline{K}^{*0} \to K^-\pi^+$) is determined by three transversity amplitudes $\mathcal{A}_L$, $\mathcal{A}_\parallel$ and $\mathcal{A}_\perp$. The relative fraction of these can be determined from the distribution of the decay products in three angles θ_1, θ_2 and φ. Here θ_1 (θ_2) is the K^+ (K^-) emission angle with respect to the direction opposite to the B_s^0 meson momentum in the K^{*0} ($\overline{K}^{*0}$) rest frame, and φ is the angle between the normals to the K^{*0} and $\overline{K}^{*0}$ decay planes in the B_s^0 rest frame [5]. We will refer generically to the θ angle from now on, unless differences between θ_1 and θ_2 become relevant for the discussion. In a time-integrated and flavor-averaged analysis, and assuming the B_s^0 mixing phase $\beta_s \approx 0$ as in the Standard Model, the angular distribution is given by [5, 21]

$$\begin{aligned} I(\theta_1, \theta_2, \varphi) &= \frac{d^3\Gamma}{d\cos\theta_1\, d\cos\theta_2\, d\varphi} \\ &= \left(\frac{1}{\Gamma_L}|\mathcal{A}_L|^2 \cos^2\theta_1 \cos^2\theta_2 \right. \\ &\quad + \frac{1}{\Gamma_L}|\mathcal{A}_\parallel|^2 \frac{1}{2}\sin^2\theta_1 \sin^2\theta_2 \cos^2\varphi \\ &\quad + \frac{1}{\Gamma_H}|\mathcal{A}_\perp|^2 \frac{1}{2}\sin^2\theta_1 \sin^2\theta_2 \sin^2\varphi \\ &\quad \left. + \frac{1}{\Gamma_L}|\mathcal{A}_L||\mathcal{A}_\parallel| \cos\delta_\parallel \frac{1}{2\sqrt{2}} \sin 2\theta_1 \sin 2\theta_2 \cos\varphi \right). \end{aligned} \tag{3}$$

We denote the polarization fractions by

$$f_k = \frac{|\mathcal{A}_k|^2}{|\mathcal{A}_L|^2 + |\mathcal{A}_\parallel|^2 + |\mathcal{A}_\perp|^2}, \quad k = L, \parallel, \perp, \tag{4}$$

and consequently $f_L + f_\parallel + f_\perp = 1$. No *CP* violation in the mixing or in the decay has been considered. The interference terms related to the $\mathcal{A}_\perp$ amplitude, both proportional to $\sin\phi_s$, have been neglected. $\Gamma_{L,H}$ are the total widths of the low and high mass eigenstates of the B_s^0 meson, respectively, and $\delta_\parallel$ is the phase difference between $\mathcal{A}_L$ and $\mathcal{A}_\parallel$. The total decay width is defined as $\Gamma = (\Gamma_L + \Gamma_H)/2$ and $\Delta\Gamma = \Gamma_L - \Gamma_H$. Note that as a consequence of time integration the relative normalization acquired by the *CP*-even and *CP*-odd terms is different. The values $\Delta\Gamma = (0.062^{+0.034}_{-0.037}) \times 10^{12}\ \text{s}^{-1}$ and $\Gamma = (0.679^{+0.012}_{-0.011}) \times 10^{12}\ \text{s}^{-1}$ [4] were used.

The detector acceptance is compatible with being constant in φ. In contrast, it has a significant dependence on the K^{*0} polarization angle θ. The two-dimensional angular acceptance function $\epsilon(\cos\theta_1, \cos\theta_2)$ was studied with a full detector simulation. It drops to nearly zero asymmetrically as $\cos\theta_{1,2}$ becomes close to ± 1, as a consequence of the minimum p and p_T of the tracks imposed by the reconstruction.

The Monte Carlo simulation of the K^{*0} acceptance was extensively cross-checked using the $B^0 \to J/\psi K^{*0}$ control channel, taking advantage of the fact that the K^{*0} polarization in this channel was measured at the B-factory experiments [22,23]. The function $\epsilon(\cos\theta_1, \cos\theta_2)$ has been projected onto the K^{*0} and $\overline{K}^{*0}$ axes separately, showing no appreciable difference, and a small average correlation, given the size of the simulated sample. We have then used the one-dimensional acceptance $\epsilon_\theta(\cos\theta)$ as the basis of our analysis, and determined it in five bins of $\cos\theta$. Since the longitudinal polarization fraction for the $B^0 \to J/\psi K^{*0}$ channel is well measured, a comparison between data and simulation is possible. Agreement was found including variations of the angular distribution with longitudinal and transverse K^{*0} momentum. In the region $\cos\theta > 0.6$ these variations were four times larger than for lower values of $\cos\theta$.

The background $\cos\theta$ distribution was studied in two 200 MeV/c^2 sidebands, defined below and above the B_s^0 signal region. Like the signal, it showed a dip close to $\cos\theta = +1$ and it was parameterized as $\epsilon_\theta \cdot (1 + \beta\cos\theta)$. A one parameter fit for β gives the result $\beta = -0.18 \pm 0.13$.

An unbinned maximum likelihood fit was then performed to the data in a ± 50 MeV/c^2 window around the B_s^0 mass, in the region $\cos\theta < 0.6$, according to the PDF

$$\begin{aligned} F(\theta_1, \theta_2, \varphi) &= (1 - \alpha)\epsilon_\theta(\theta_1)\epsilon_\theta(\theta_2) I(\theta_1, \theta_2, \varphi) \\ &\quad + \alpha(1 + \beta\cos\theta_1)(1 + \beta\cos\theta_2)\epsilon_\theta(\theta_1)\epsilon_\theta(\theta_2). \end{aligned} \tag{5}$$

The background fraction α was determined from the fit to the B_s^0 mass spectrum described in Section 2. Only three parameters were allowed to vary in the fit, namely f_L, $f_\parallel$ and the phase difference $\delta_\parallel$.

One-dimensional projections of the fit results are shown in Fig. 4. The consistency of the measurement in various regions of the K^{*0} phase space, and of the impact parameter of the daughter particles, was checked. The experimental systematic error on f_L was estimated from the variation of the measurements amongst those regions to be ± 0.03.

The acceptance for $B_s^0 \to K^{*0}\overline{K}^{*0}$ is not uniform as a function of proper decay time due to the cuts made on the IP of the kaons and pions, and a small correction to the polarization fractions, of order 3%, was applied in order to take into account this effect. It was calculated from the variation in the measured polarization amplitudes induced by including a parametrization of the time acceptance in Eq. (5). Note the different correction sign for each polarization fraction, as a consequence of the assumption $\Delta\Gamma \neq 0$.

The sensitivity of the f_L measurement with respect to small variations of the $\cos\theta$ distribution has been tested. These variations could be attributed to experimental errors not accounted for in the simulation or to interference with other partial waves in the $K\pi$ system. A high statistics study using $B^0 \to J/\psi K^{*0}$ muon triggers revealed a small systematic difference between data and simulation in $\epsilon_\theta(\cos\theta)$ as $\cos\theta$ approaches $+1$, which was taken into account as a correction in our analysis. When this correction

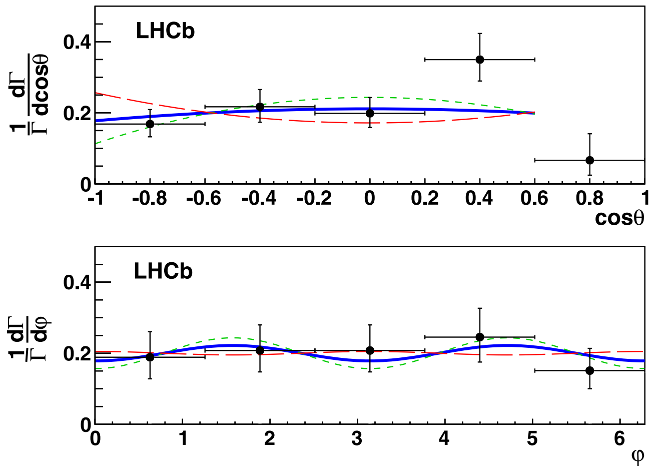

Fig. 4. $\cos\theta$ (above) and φ (below) acceptance corrected distributions for events in the narrow window around the B_s^0 mass. The blue line is the projection of the fit model given by Eq. (3) for the measured values of the parameters f_L, $f_\parallel$ and $\delta_\parallel$. The dotted lines indicate $\pm 1\sigma$ variation of the f_L central value. (For interpretation of the references to color in this figure legend, the reader is referred to the web version of this Letter.)

in varied by $\pm 100\%$, f_L varies by ± 0.02 which we consider as an additional source of systematic error. The total systematic on f_L is thus ± 0.04.

We finally measure the K^{*0} longitudinal polarization fraction $f_L = 0.31 \pm 0.12(\text{stat.}) \pm 0.04(\text{syst.})$, as well as the transverse components $f_\parallel$ and $f_\perp$. In the small sample available, the *CP*-odd component $f_\perp$ appears to be sizable $f_\perp = 0.38 \pm 0.11(\text{stat.}) \pm 0.04(\text{syst.})$. A significant measurement of $\delta_\parallel$ could not be achieved ($\delta_\parallel = 1.47 \pm 1.85$).

As seen in Eq. (3), due to a nonzero $\Delta\Gamma$ time integration changes the relative proportion between the various terms of the angular distribution, with respect to their values at $t = 0$. If we call f_k^0 the polarization fractions we would have measured under the assumption $\Delta\Gamma = 0$, it can be derived from Eq. (3) that our measured values are

$$f_k = f_k^0\left(1 + \eta_k \frac{\Delta\Gamma}{2\Gamma}\right) \tag{6}$$

with CP eigenvalue $\eta_k = +1, +1, -1$ for $k = L, \parallel, \perp$. Given the current knowledge of $\Delta\Gamma/\Gamma$ [4], the magnitude of the correction to f_k amounts to 4.6%, and the associated systematic error related to $\Delta\Gamma$ error is 2.6%, which we have neglected in comparison to other sources.

5. Determination of the branching fraction

The results of the previous sections can be brought together to provide a determination of the branching fraction of the $B_s^0 \to K^{*0}\overline{K}^{*0}$ decay based upon the use of the normalization channel $B^0 \to J/\psi K^{*0}$ through the expression

$$\begin{aligned}\mathcal{B}\big(B_s^0 \to K^{*0}\overline{K}^{*0}\big) = \lambda_{f_L} \times \frac{\epsilon^{sel}_{B^0\to J/\psi K^{*0}}}{\epsilon^{sel}_{B_s^0\to K^{*0}\overline{K}^{*0}}} \\ \times \frac{\epsilon^{trig}_{B^0\to J/\psi K^{*0}}}{\epsilon^{trig}_{B_s^0\to K^{*0}\overline{K}^{*0}}} \times \frac{N_{B_s^0\to K^{*0}\overline{K}^{*0}}}{N_{B^0\to J/\psi K^{*0}}} \\ \times \mathcal{B}_{vis}\big(B^0 \to J/\psi K^{*0}\big) \times \frac{f_d}{f_s} \times \frac{9}{4},\end{aligned} \tag{7}$$

where $\mathcal{B}_{vis}(B^0 \to J/\psi K^{*0})$, the visible branching ratio, is the product $\mathcal{B}(B^0 \to J/\psi K^{*0}) \times \mathcal{B}(J/\psi \to \mu^+\mu^-) \times \mathcal{B}(K^{*0} \to K^+\pi^-)$. The numerical value of $\mathcal{B}(B^0 \to J/\psi K^{*0}) = (1.33 \pm 0.06) \times 10^{-3}$ is taken from the world average in [4], $\mathcal{B}(J/\psi \to \mu^+\mu^-) = 0.0593 \pm 0.0006$ [4] and $\mathcal{B}(K^{*0} \to K^+\pi^-) = 2/3$ [4]. The ratio of *b*-quark hadronization factors that accounts for the different production rate of B^0 and B_s^0 mesons is $f_s/f_d = 0.253 \pm 0.031$ [24]. The factor 9/4 is the inverse square of the 2/3 branching fraction of $K^{*0} \to K^+\pi^-$. The number of candidate events in the signal and control channel data samples are designated by $N_{B_s^0\to K^{*0}\overline{K}^{*0}}$ and $N_{B^0\to J/\psi K^{*0}}$.

The correction factor λ_{f_L} is motivated by the fact that the overall efficiency of the LHCb detector is a linear function of the K^{*0} longitudinal polarization f_L. Taking into account the measured value and errors reported in Section 4, Monte Carlo simulation was used to estimate $\lambda_{f_L} = 0.812 \pm 0.059$.

We have considered two sources of systematic uncertainty associated to the ratio of selection efficiencies. The first source results from discrepancies between data and simulation in the variables related to track and vertex quality, and the second is related to particle identification. A small difference observed in the average impact parameter of the particles was corrected for by introducing an additional smearing to the track parameters in the simulation [25]. While the absolute efficiencies vary significantly as a function of vertex resolution, the ratio of efficiencies remains stable. We have assigned a 2% uncertainty to the ratio, after comparison between simulation and the $B^0 \to J/\psi K^{*0}$ data. The K/π identification efficiency was determined using a sample of $B^0 \to J/\psi K^{*0}$ events selected without making use of the RICH detectors. As the signal channel contains one more kaon than the control channel, a correction factor of 1.098 ± 0.019 was applied to the branching fraction, and a 2% error was assigned to it. The efficiency of muon identification agrees with simulation within 1.1% [26]. All these factors are combined to produce an overall systematic uncertainty of 3.4% in the ratio of selection efficiencies. The uncertainty in the background model in the B_s^0 mass fit (± 2 events) contributes an additional systematic error of 4.7%.

Trigger efficiencies can be determined, for particular trigger paths in LHCb, using the data driven algorithm described in [26]. This algorithm could be applied for the specific hadronic triggers used for $B^0 \to J/\psi K^{*0}$, but not for the small $B_s^0 \to K^{*0}\overline{K}^{*0}$ signal. The efficiency related to cuts on global event properties, applied during the 2010 data taking, is determined from J/ψ minimum bias triggers [26]. The result indicates a trigger efficiency of $(26.8 \pm 3.8)\%$, smaller than the simulation result of $(31.16 \pm 0.63)\%$ shown in Table 2. Although these are consistent within uncertainties, we nonetheless apply a -9% correction to the ratio of trigger efficiencies between $B^0 \to J/\psi K^{*0}$ and $B_s^0 \to K^{*0}\overline{K}^{*0}$ channels, taking into account correlations in the trigger probability. A systematic error of 11% was assigned to uncertainty on the trigger efficiency, entirely limited by statistics, both in the signal and control channels. Detector occupancies, estimated by the average number of reconstructed tracks, are larger by 10% in the data than in the simulation. This implies an additional correction of +4.5% to the ratio of efficiencies, since the control channel is observed to be more sensitive to occupancy than the signal channel.

An ~8% S-wave contribution under the K^{*0} resonance in the $B^0 \to J/\psi K^{*0}$ channel has been observed by BaBar [23], and the data in a ± 70 MeV/c^2 mass interval around the K^{*0} mass [27] yields a $(9.0 \pm 3.6)\%$ extrapolation to the ± 150 MeV/c^2 mass window. The S-wave background doubles for the $K^{*0}\overline{K}^{*0}$ final state, and it may certainly have a different coupling for both channels. Our direct measurement reported in Section 2 of $(19 \pm 9)\%$ is still lacking precision to be used for this purpose. When evaluating the

Table 3
Estimated systematic error sources in the $\mathcal{B}(B_s^0 \to K^{*0}\overline{K}^{*0})$ measurement.

Systematic effect	Error (%)
Trigger efficiency	11.0
Global angular acceptance	7.2
S-wave fraction	5.0
Background subtraction	4.7
$B^0 \to J/\psi K^{*0}$ and $J/\psi \to \mu\mu$ BR uncertainty	4.6
Selection efficiency	3.4
Total	15.9

branching fraction, we have assumed a 9% S-wave contribution, and assigned a systematic error of 50% to this hypothesis. A summary of the various contributions to the systematic error can be seen in Table 3.

Our final result is

$$\mathcal{B}\big(B_s^0 \to K^{*0}\overline{K}^{*0}\big) = \big(2.81 \pm 0.46(\text{stat.}) \pm 0.45(\text{syst.}) \pm 0.34(f_s/f_d)\big) \times 10^{-5}.$$

As we have seen at the end of Section 4, unequal normalization factors arise upon time integration of individual polarization amplitudes with well-defined *CP*-eigenvalues. This has the interesting implication that the time-integrated flavor-averaged branching fraction (B_1) as determined above cannot be directly compared with theoretical predictions solely formulated in terms of the decay amplitudes ${\mathcal{A}_L}^2 + {\mathcal{A}_\parallel}^2 + {\mathcal{A}_\perp}^2$ (B_0). Meson oscillation needs to be taken into account, since two distinct particles with different lifetimes are involved. Owing to the fact that $\mathcal{A}_\perp$ is *CP*-odd, the relationship between these quantities reads as follows

$$B_0 = B_1\left(1 + \frac{\Delta\Gamma}{2\Gamma}(f_L + f_\parallel - f_\perp)\right). \tag{8}$$

According to our measurements of $f_L + f_\parallel - f_\perp$, the correction is small (3% if current values are taken for $\Delta\Gamma$), and we do not apply it to our measurement.

6. Conclusion

The $b \to s$ penguin decay $B_s^0 \to K^{*0}\overline{K}^{*0}$ has been observed for the first time. Using 35 pb^{-1} of *pp* collisions at 7 TeV centre-of-mass energy, LHCb has found 49.8 ± 7.5 signal events in the mass interval $\pm 50\ \text{MeV}/c^2$ around the B_s^0 mass. Analysis of the $K^+\pi^-$ mass distributions shows that most of the signal comes from $B_s^0 \to K^{*0}\overline{K}^{*0}$, with some S-wave contribution. The branching fraction has been measured, with the result $\mathcal{B}(B_s^0 \to K^{*0}\overline{K}^{*0}) = (2.81 \pm 0.46(\text{stat.}) \pm 0.45(\text{syst.}) \pm 0.34(f_s/f_d)) \times 10^{-5}$. The *CP*-averaged longitudinal K^{*0} polarization fraction has also been measured to be $f_L = 0.31 \pm 0.12(\text{stat.}) \pm 0.04(\text{syst.})$, as well as the *CP*-odd component $f_\perp = 0.38 \pm 0.11(\text{stat.}) \pm 0.04(\text{syst.})$.

When we consider our measurement in association with that of [9], it is remarkable that the longitudinal polarization of the K^{*0} mesons seems to be quite different between $B_s^0 \to K^{*0}\overline{K}^{*0}$ ($f_L = 0.31 \pm 0.12(\text{stat.}) \pm 0.04(\text{syst.})$) and $B^0 \to K^{*0}\overline{K}^{*0}$ ($f_L = 0.80^{+0.10}_{-0.12}(\text{stat.}) \pm 0.06(\text{syst.})$), despite the fact that the two decays are related by a U-spin rotation. However, the ratio of the branching ratios of B_s^0 and B^0 decays is consistent with $1/\lambda^2$ where λ is the Wolfenstein parameter, as expected.

Acknowledgements

We would like to thank J. Matías for useful discussions. We express our gratitude to our colleagues in the CERN accelerator departments for the excellent performance of the LHC. We thank the technical and administrative staff at CERN and at the LHCb institutes, and acknowledge support from the National Agencies: National Agencies: CAPES, CNPq, FAPERJ and FINEP (Brazil); CERN; NSFC (China); CNRS/IN2P3 (France); BMBF, DFG, HGF and MPG (Germany); SFI (Ireland); INFN (Italy); FOM and NWO (The Netherlands); SCSR (Poland); ANCS (Romania); MinES of Russia and Rosatom (Russia); MICINN, XuntaGal and GENCAT (Spain); SNSF and SER (Switzerland); NAS Ukraine (Ukraine); STFC (United Kingdom); NSF (USA). We also acknowledge the support received from the ERC under FP7 and the Region Auvergne.

Open access

References

[1] M. Beneke, J. Rohrer, D. Yang, Nucl. Phys. B 774 (2007) 64.
[2] BaBar Collaboration, B. Aubert, et al., Phys. Rev. Lett. 93 (2004) 231804.
[3] Belle Collaboration, K.F. Chen, et al., Phys. Rev. Lett 94 (2005) 221804.
[4] Particle Data Group, K. Nakamura, et al., J. Phys. G 37 (2010) 075021.
[5] S. Descotes-Genon, J. Matias, J. Virto, Phys. Rev. D 76 (2007) 074005.
[6] M. Ciuchini, M. Pierini, L. Silvestrini, Phys. Rev. Lett. 100 (2008) 031802.
[7] R. Fleischer, M. Gronau, Phys. Lett. B 660 (2008) 212.
[8] R. Fleischer, Phys. Rev. D 60 (1999) 073008.
[9] BaBar Collaboration, B. Aubert, et al., Phys. Rev. Lett. 100 (2008) 081801.
[10] SLD Collaboration, K. Abe, et al., Phys. Rev. D 62 (2000) 071101.
[11] LHCb Collaboration, A.A. Alves Jr., et al., JINST 3 (2008) S08005.
[12] LHCb Collaboration, LHCb-PUB-2011-017, 2011.
[13] D. Karlen, Comput. Phys. 12 (1998) 380.
[14] D. Martínez Santos, CERN-THESIS-2010-068, PhD thesis, Universidade de Santiago de Compostela, 2010.
[15] D.J. Lange, Nucl. Instrum. Methods A 462 (2001) 152.
[16] S. Torbjorn, et al., JHEP 0605 (2006) 026.
[17] GEANT4 Collaboration, S. Agostinelli, et al., Nucl. Instrum. Methods A 506 (2003) 250.
[18] J. Podolanski, R. Armenteros, Phil. Mag. 45 (1954) 13.
[19] P. Koppenburg, PhD thesis, Université de Lausanne, 2002.
[20] T. Skwarnicki, DESY F31-86-02 1986, PhD thesis, Institute of Nuclear Physics, Krakow, 1986.
[21] I. Dunietz, R. Fleischer, U. Nierste, Phys. Rev. D 63 (2001) 114015.
[22] Belle Collaboration, K. Abe, et al., Phys. Lett. B 538 (2002) 11.
[23] BaBar Collaboration, B. Aubert, et al., Phys. Rev. D 76 (2007) 031102.
[24] LHCb Collaboration, R. Aaij, et al., Phys. Rev. Lett. 107 (2011) 211801.
[25] LHCb Collaboration, R. Aaij, et al., Phys. Lett. B 699 (2011) 330.
[26] LHCb Collaboration, R. Aaij, et al., Eur. Phys. J. C 71 (2011) 1645.
[27] LHCb Collaboration, CERN-LHCb-CONF-2011-002, 2011.

LHCb Collaboration

R. Aaij [23], C. Abellan Beteta [35,n], B. Adeva [36,*], M. Adinolfi [42], C. Adrover [6], A. Affolder [48], Z. Ajaltouni [5], J. Albrecht [37], F. Alessio [37], M. Alexander [47], G. Alkhazov [29], P. Alvarez Cartelle [36], A.A. Alves Jr. [22], S. Amato [2], Y. Amhis [38], J. Anderson [39], R.B. Appleby [50], O. Aquines Gutierrez [10], F. Archilli [18,37], L. Arrabito [53], A. Artamonov [34], M. Artuso [52,37], E. Aslanides [6], G. Auriemma [22,m], S. Bachmann [11], J.J. Back [44], D.S. Bailey [50], V. Balagura [30,37], W. Baldini [16], R.J. Barlow [50], C. Barschel [37], S. Barsuk [7], W. Barter [43], A. Bates [47], C. Bauer [10], Th. Bauer [23], A. Bay [38], I. Bediaga [1], S. Belogurov [30], K. Belous [34], I. Belyaev [30,37], E. Ben-Haim [8], M. Benayoun [8], G. Bencivenni [18], S. Benson [46], J. Benton [42], R. Bernet [39], M.-O. Bettler [17], M. van Beuzekom [23], A. Bien [11], S. Bifani [12], A. Bizzeti [17,h], P.M. Bjørnstad [50], T. Blake [37], F. Blanc [38], C. Blanks [49], J. Blouw [11], S. Blusk [52], A. Bobrov [33], V. Bocci [22], A. Bondar [33], N. Bondar [29], W. Bonivento [15], S. Borghi [47], A. Borgia [52], T.J.V. Bowcock [48], C. Bozzi [16], T. Brambach [9], J. van den Brand [24], J. Bressieux [38], D. Brett [50], S. Brisbane [51], M. Britsch [10], T. Britton [52], N.H. Brook [42], H. Brown [48], A. Büchler-Germann [39], I. Burducea [28], A. Bursche [39], J. Buytaert [37], S. Cadeddu [15], J.M. Caicedo Carvajal [37], O. Callot [7], M. Calvi [20,j], M. Calvo Gomez [35,n], A. Camboni [35], P. Campana [18,37], A. Carbone [14], G. Carboni [21,k], R. Cardinale [19,37,i], A. Cardini [15], L. Carson [36], K. Carvalho Akiba [2], G. Casse [48], M. Cattaneo [37], M. Charles [51], Ph. Charpentier [37], N. Chiapolini [39], K. Ciba [37], X. Cid Vidal [36], G. Ciezarek [49], P.E.L. Clarke [46,37], M. Clemencic [37], H.V. Cliff [43], J. Closier [37], C. Coca [28], V. Coco [23], J. Cogan [6], P. Collins [37], A. Comerma-Montells [35], F. Constantin [28], G. Conti [38], A. Contu [51], A. Cook [42], M. Coombes [42], G. Corti [37], G.A. Cowan [38], R. Currie [46], B. D'Almagne [7], C. D'Ambrosio [37], P. David [8], I. De Bonis [4], S. De Capua [21,k], M. De Cian [39], F. De Lorenzi [12], J.M. De Miranda [1], L. De Paula [2], P. De Simone [18], D. Decamp [4], M. Deckenhoff [9], H. Degaudenzi [38,37], M. Deissenroth [11], L. Del Buono [8], C. Deplano [15], D. Derkach [14,37], O. Deschamps [5], F. Dettori [24], J. Dickens [43], H. Dijkstra [37], P. Diniz Batista [1], F. Domingo Bonal [35,n], S. Donleavy [48], F. Dordei [11], A. Dosil Suárez [36], D. Dossett [44], A. Dovbnya [40], F. Dupertuis [38], R. Dzhelyadin [34], A. Dziurda [25], S. Easo [45], U. Egede [49], V. Egorychev [30], S. Eidelman [33], D. van Eijk [23], F. Eisele [11], S. Eisenhardt [46], R. Ekelhof [9], L. Eklund [47], Ch. Elsasser [39], D. Esperante Pereira [36], L. Estève [43], A. Falabella [16,e], E. Fanchini [20,j], C. Färber [11], G. Fardell [46], C. Farinelli [23], S. Farry [12], V. Fave [38], V. Fernandez Albor [36], M. Ferro-Luzzi [37], S. Filippov [32], C. Fitzpatrick [46], M. Fontana [10], F. Fontanelli [19,i], R. Forty [37], M. Frank [37], C. Frei [37], M. Frosini [17,37,f], S. Furcas [20], A. Gallas Torreira [36], D. Galli [14,c], M. Gandelman [2], P. Gandini [51], Y. Gao [3], J.-C. Garnier [37], J. Garofoli [52], J. Garra Tico [43], L. Garrido [35], D. Gascon [35], C. Gaspar [37], N. Gauvin [38], M. Gersabeck [37], T. Gershon [44,37], Ph. Ghez [4], A. Giachero [20], V. Gibson [43], V.V. Gligorov [37], C. Göbel [54], D. Golubkov [30], A. Golutvin [49,30,37], A. Gomes [2], H. Gordon [51], M. Grabalosa Gándara [35], R. Graciani Diaz [35], L.A. Granado Cardoso [37], E. Graugés [35], G. Graziani [17], A. Grecu [28], E. Greening [51], S. Gregson [43], B. Gui [52], E. Gushchin [32], Yu. Guz [34], T. Gys [37], G. Haefeli [38], C. Haen [37], S.C. Haines [43], T. Hampson [42], S. Hansmann-Menzemer [11], R. Harji [49], N. Harnew [51], J. Harrison [50], P.F. Harrison [44], J. He [7], V. Heijne [23], K. Hennessy [48], P. Henrard [5], J.A. Hernando Morata [36], E. van Herwijnen [37], E. Hicks [48], K. Holubyev [11], P. Hopchev [4], W. Hulsbergen [23], P. Hunt [51], T. Huse [48], R.S. Huston [12], D. Hutchcroft [48], D. Hynds [47], V. Iakovenko [41], P. Ilten [12], J. Imong [42], R. Jacobsson [37], A. Jaeger [11], M. Jahjah Hussein [5], E. Jans [23], F. Jansen [23], P. Jaton [38], B. Jean-Marie [7], F. Jing [3], M. John [51], D. Johnson [51], C.R. Jones [43], B. Jost [37], M. Kaballo [9], S. Kandybei [40], M. Karacson [37], T.M. Karbach [9], J. Keaveney [12], U. Kerzel [37], T. Ketel [24], A. Keune [38], B. Khanji [6], Y.M. Kim [46], M. Knecht [38], P. Koppenburg [23], A. Kozlinskiy [23], L. Kravchuk [32], K. Kreplin [11], M. Kreps [44], G. Krocker [11], P. Krokovny [11], F. Kruse [9], K. Kruzelecki [37], M. Kucharczyk [20,25,37,j], R. Kumar [14,37], T. Kvaratskheliya [30,37], V.N. La Thi [38], D. Lacarrere [37], G. Lafferty [50], A. Lai [15], D. Lambert [46], R.W. Lambert [37], E. Lanciotti [37], G. Lanfranchi [18], C. Langenbruch [11], T. Latham [44], R. Le Gac [6], J. van Leerdam [23], J.-P. Lees [4], R. Lefèvre [5], A. Leflat [31,37], J. Lefrançois [7], O. Leroy [6], T. Lesiak [25], L. Li [3], L. Li Gioi [5], M. Lieng [9], M. Liles [48], R. Lindner [37], C. Linn [11], B. Liu [3], G. Liu [37], J.H. Lopes [2], E. Lopez Asamar [35], N. Lopez-March [38], J. Luisier [38], F. Machefert [7], I.V. Machikhiliyan [4,30], F. Maciuc [10], O. Maev [29,37], J. Magnin [1], S. Malde [51], R.M.D. Mamunur [37], G. Manca [15,d], G. Mancinelli [6], N. Mangiafave [43], U. Marconi [14], R. Märki [38], J. Marks [11], G. Martellotti [22], A. Martens [7], L. Martin [51], A. Martín Sánchez [7], D. Martinez Santos [37], A. Massafferri [1], Z. Mathe [12], C. Matteuzzi [20], M. Matveev [29], E. Maurice [6], B. Maynard [52], A. Mazurov [16,32,37], G. McGregor [50], R. McNulty [12], C. Mclean [14], M. Meissner [11], M. Merk [23], J. Merkel [9], R. Messi [21,k], S. Miglioranzi [37], D.A. Milanes [13,37], M.-N. Minard [4], S. Monteil [5], D. Moran [12], P. Morawski [25], R. Mountain [52], I. Mous [23], F. Muheim [46], K. Müller [39], R. Muresan [28,38], B. Muryn [26], M. Musy [35], J. Mylroie-Smith [48], P. Naik [42], T. Nakada [38], R. Nandakumar [45], I. Nasteva [1], M. Nedos [9], M. Needham [46], N. Neufeld [37], C. Nguyen-Mau [38,o], M. Nicol [7], S. Nies [9], V. Niess [5], N. Nikitin [31], A. Nomerotski [51], A. Novoselov [34], A. Oblakowska-Mucha [26], V. Obraztsov [34], S. Oggero [23], S. Ogilvy [47], O. Okhrimenko [41], R. Oldeman [15,d], M. Orlandea [28], J.M. Otalora Goicochea [2], P. Owen [49], K. Pal [52], J. Palacios [39], A. Palano [13,b], M. Palutan [18],

J. Panman[37], A. Papanestis[45], M. Pappagallo[13,b], C. Parkes[47,37], C.J. Parkinson[49], G. Passaleva[17], G.D. Patel[48], M. Patel[49], S.K. Paterson[49], G.N. Patrick[45], C. Patrignani[19,i], C. Pavel-Nicorescu[28], A. Pazos Alvarez[36], A. Pellegrino[23], G. Penso[22,l], M. Pepe Altarelli[37], S. Perazzini[14,c], D.L. Perego[20,j], E. Perez Trigo[36], A. Pérez-Calero Yzquierdo[35], P. Perret[5], M. Perrin-Terrin[6], A. Petrella[16,37], A. Petrolini[19,i], A. Phan[52], E. Picatoste Olloqui[35], B. Pie Valls[35], B. Pietrzyk[4], T. Pilar[44], D. Pinci[22], R. Plackett[47], S. Playfer[46], M. Plo Casasus[36], G. Polok[25], A. Poluektov[44,33], E. Polycarpo[2], D. Popov[10], B. Popovici[28], C. Potterat[35], A. Powell[51], T. du Pree[23], J. Prisciandaro[38], V. Pugatch[41], A. Puig Navarro[35], W. Qian[52], J.H. Rademacker[42], B. Rakotomiaramanana[38], M.S. Rangel[2], I. Raniuk[40], G. Raven[24], S. Redford[51], M.M. Reid[44], A.C. dos Reis[1], S. Ricciardi[45], K. Rinnert[48], D.A. Roa Romero[5], P. Robbe[7], E. Rodrigues[47], F. Rodrigues[2], P. Rodriguez Perez[36], G.J. Rogers[43], S. Roiser[37], V. Romanovsky[34], M. Rosello[35,n], J. Rouvinet[38], T. Ruf[37], H. Ruiz[35], G. Sabatino[21,k], J.J. Saborido Silva[36], N. Sagidova[29], P. Sail[47], B. Saitta[15,d], C. Salzmann[39], M. Sannino[19,i], R. Santacesaria[22], C. Santamarina Rios[36], R. Santinelli[37], E. Santovetti[21,k], M. Sapunov[6], A. Sarti[18,l], C. Satriano[22,m], A. Satta[21], M. Savrie[16,e], D. Savrina[30], P. Schaack[49], M. Schiller[24], S. Schleich[9], M. Schmelling[10], B. Schmidt[37], O. Schneider[38], A. Schopper[37], M.-H. Schune[7], R. Schwemmer[37], B. Sciascia[18], A. Sciubba[18,l], M. Seco[36], A. Semennikov[30], K. Senderowska[26], I. Sepp[49], N. Serra[39], J. Serrano[6], P. Seyfert[11], B. Shao[3], M. Shapkin[34], I. Shapoval[40,37], P. Shatalov[30], Y. Shcheglov[29], T. Shears[48], L. Shekhtman[33], O. Shevchenko[40], V. Shevchenko[30], A. Shires[49], R. Silva Coutinho[54], H.P. Skottowe[43], T. Skwarnicki[52], A.C. Smith[37], N.A. Smith[48], E. Smith[51,45], K. Sobczak[5], F.J.P. Soler[47], A. Solomin[42], F. Soomro[18], B. Souza De Paula[2], B. Spaan[9], A. Sparkes[46], P. Spradlin[47], F. Stagni[37], S. Stahl[11], O. Steinkamp[39], S. Stoica[28], S. Stone[52,37], B. Storaci[23], M. Straticiuc[28], U. Straumann[39], N. Styles[46], V.K. Subbiah[37], S. Swientek[9], M. Szczekowski[27], P. Szczypka[38], T. Szumlak[26], S. T'Jampens[4], E. Teodorescu[28], F. Teubert[37], C. Thomas[51], E. Thomas[37], J. van Tilburg[11], V. Tisserand[4], M. Tobin[39], S. Topp-Joergensen[51], N. Torr[51], E. Tournefier[4,49], M.T. Tran[38], A. Tsaregorodtsev[6], N. Tuning[23], M. Ubeda Garcia[37], A. Ukleja[27], P. Urquijo[52], U. Uwer[11], V. Vagnoni[14], G. Valenti[14], R. Vazquez Gomez[35], P. Vazquez Regueiro[36], S. Vecchi[16], J.J. Velthuis[42], M. Veltri[17,g], K. Vervink[37], B. Viaud[7], I. Videau[7], X. Vilasis-Cardona[35,n], J. Visniakov[36], A. Vollhardt[39], D. Voong[42], A. Vorobyev[29], H. Voss[10], K. Wacker[9], S. Wandernoth[11], J. Wang[52], D.R. Ward[43], A.D. Webber[50], D. Websdale[49], M. Whitehead[44], D. Wiedner[11], L. Wiggers[23], G. Wilkinson[51], M.P. Williams[44,45], M. Williams[49], F.F. Wilson[45], J. Wishahi[9], M. Witek[25], W. Witzeling[37], S.A. Wotton[43], K. Wyllie[37], Y. Xie[46], F. Xing[51], Z. Xing[52], Z. Yang[3], R. Young[46], O. Yushchenko[34], M. Zavertyaev[10,a], F. Zhang[3], L. Zhang[52], W.C. Zhang[12], Y. Zhang[3], A. Zhelezov[11], L. Zhong[3], E. Zverev[31], A. Zvyagin[37]

[1] *Centro Brasileiro de Pesquisas Físicas (CBPF), Rio de Janeiro, Brazil*
[2] *Universidade Federal do Rio de Janeiro (UFRJ), Rio de Janeiro, Brazil*
[3] *Center for High Energy Physics, Tsinghua University, Beijing, China*
[4] *LAPP, Université de Savoie, CNRS/IN2P3, Annecy-Le-Vieux, France*
[5] *Clermont Université, Université Blaise Pascal, CNRS/IN2P3, LPC, Clermont-Ferrand, France*
[6] *CPPM, Aix-Marseille Université, CNRS/IN2P3, Marseille, France*
[7] *LAL, Université Paris-Sud, CNRS/IN2P3, Orsay, France*
[8] *LPNHE, Université Pierre et Marie Curie, Université Paris Diderot, CNRS/IN2P3, Paris, France*
[9] *Fakultät Physik, Technische Universität Dortmund, Dortmund, Germany*
[10] *Max-Planck-Institut für Kernphysik (MPIK), Heidelberg, Germany*
[11] *Physikalisches Institut, Ruprecht-Karls-Universität Heidelberg, Heidelberg, Germany*
[12] *School of Physics, University College Dublin, Dublin, Ireland*
[13] *Sezione INFN di Bari, Bari, Italy*
[14] *Sezione INFN di Bologna, Bologna, Italy*
[15] *Sezione INFN di Cagliari, Cagliari, Italy*
[16] *Sezione INFN di Ferrara, Ferrara, Italy*
[17] *Sezione INFN di Firenze, Firenze, Italy*
[18] *Laboratori Nazionali dell'INFN di Frascati, Frascati, Italy*
[19] *Sezione INFN di Genova, Genova, Italy*
[20] *Sezione INFN di Milano Bicocca, Milano, Italy*
[21] *Sezione INFN di Roma Tor Vergata, Roma, Italy*
[22] *Sezione INFN di Roma La Sapienza, Roma, Italy*
[23] *Nikhef National Institute for Subatomic Physics, Amsterdam, Netherlands*
[24] *Nikhef National Institute for Subatomic Physics and Vrije Universiteit, Amsterdam, Netherlands*
[25] *Henryk Niewodniczanski Institute of Nuclear Physics Polish Academy of Sciences, Cracow, Poland*
[26] *Faculty of Physics & Applied Computer Science, Cracow, Poland*
[27] *Soltan Institute for Nuclear Studies, Warsaw, Poland*
[28] *Horia Hulubei National Institute of Physics and Nuclear Engineering, Bucharest-Magurele, Romania*
[29] *Petersburg Nuclear Physics Institute (PNPI), Gatchina, Russia*
[30] *Institute of Theoretical and Experimental Physics (ITEP), Moscow, Russia*

[31] *Institute of Nuclear Physics, Moscow State University (SINP MSU), Moscow, Russia*
[32] *Institute for Nuclear Research of the Russian Academy of Sciences (INR RAN), Moscow, Russia*
[33] *Budker Institute of Nuclear Physics (SB RAS) and Novosibirsk State University, Novosibirsk, Russia*
[34] *Institute for High Energy Physics (IHEP), Protvino, Russia*
[35] *Universitat de Barcelona, Barcelona, Spain*
[36] *Universidad de Santiago de Compostela, Santiago de Compostela, Spain*
[37] *European Organization for Nuclear Research (CERN), Geneva, Switzerland*
[38] *Ecole Polytechnique Fédérale de Lausanne (EPFL), Lausanne, Switzerland*
[39] *Physik-Institut, Universität Zürich, Zürich, Switzerland*
[40] *NSC Kharkiv Institute of Physics and Technology (NSC KIPT), Kharkiv, Ukraine*
[41] *Institute for Nuclear Research of the National Academy of Sciences (KINR), Kyiv, Ukraine*
[42] *H.H. Wills Physics Laboratory, University of Bristol, Bristol, United Kingdom*
[43] *Cavendish Laboratory, University of Cambridge, Cambridge, United Kingdom*
[44] *Department of Physics, University of Warwick, Coventry, United Kingdom*
[45] *STFC Rutherford Appleton Laboratory, Didcot, United Kingdom*
[46] *School of Physics and Astronomy, University of Edinburgh, Edinburgh, United Kingdom*
[47] *School of Physics and Astronomy, University of Glasgow, Glasgow, United Kingdom*
[48] *Oliver Lodge Laboratory, University of Liverpool, Liverpool, United Kingdom*
[49] *Imperial College London, London, United Kingdom*
[50] *School of Physics and Astronomy, University of Manchester, Manchester, United Kingdom*
[51] *Department of Physics, University of Oxford, Oxford, United Kingdom*
[52] *Syracuse University, Syracuse, NY, United States*
[53] *CC-IN2P3, CNRS/IN2P3, Lyon-Villeurbanne, France* [p]
[54] *Pontifícia Universidade Católica do Rio de Janeiro (PUC-Rio), Rio de Janeiro, Brazil* [q]

* Corresponding author.
E-mail address: Bernardo.Adeva@usc.es (B. Adeva).
[a] P.N. Lebedev Physical Institute, Russian Academy of Science (LPI RAS), Moscow, Russia.
[b] Università di Bari, Bari, Italy.
[c] Università di Bologna, Bologna, Italy.
[d] Università di Cagliari, Cagliari, Italy.
[e] Università di Ferrara, Ferrara, Italy.
[f] Università di Firenze, Firenze, Italy.
[g] Università di Urbino, Urbino, Italy.
[h] Università di Modena e Reggio Emilia, Modena, Italy.
[i] Università di Genova, Genova, Italy.
[j] Università di Milano Bicocca, Milano, Italy.
[k] Università di Roma Tor Vergata, Roma, Italy.
[l] Università di Roma La Sapienza, Roma, Italy.
[m] Università della Basilicata, Potenza, Italy.
[n] LIFAELS, La Salle, Universitat Ramon Llull, Barcelona, Spain.
[o] Hanoi University of Science, Hanoi, Viet Nam.
[p] Associated member.
[q] Associated to Universidade Federal do Rio de Janeiro (UFRJ), Rio de Janeiro, Brazil.